

# Classification of atmospheric river events on the U.S. west coast using a trajectory model



Ju-Mee Ryo<sup>1</sup>, Duane E. Waliser<sup>2</sup>, Darryn W. Waugh<sup>4</sup>, Sun Wong<sup>2</sup>, Eric J. Fetzer<sup>2</sup>, Inez Fung<sup>5</sup>

<sup>1</sup> Atmospheric Science Branch, NASA Ames Research Center, <sup>2</sup> Jet Propulsion Laboratory, California Institute of Technology, <sup>4</sup> Department of Earth and Planetary Sciences, Johns Hopkins University, <sup>5</sup> Department of Earth and Planetary Sciences, University of California, Berkeley.

## Introduction

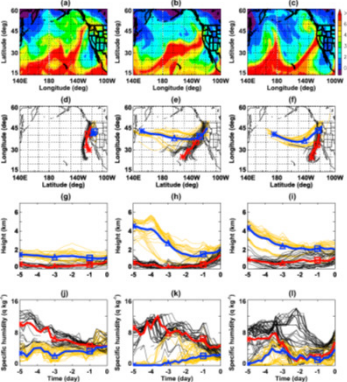
- One of the challenging problems in understanding Atmospheric River (AR) events is their apparent "randomness" and "variability". We characterize AR events into a small set of sensible types and obtain common characteristics in terms of their water vapor origins and pathways to understanding these "random" events.
- We also investigate the role of upper level PV on AR events over the west coast of the U.S.

## Data and Method

- DATA:** Historical AR events (1997-2010) records, NASA Goddard trajectory model (Schoeberl and Spurling [1995], and later modified by Wright et al. [2011] and Huang et al. [2012]). Global Modeling Assimilation Office Modern Era Retrospective-analysis for Research and Applications (GMAO MERRA) (Suarez et al., 2008; Bosilovich et al., 2008, 2011; Rienecker et al., 2011), and observed Climate Prediction Center (CPC) hydrologic data (Higgins et al., 2000).
- Method:** K-mean clustering method in order to classify the trajectories. To remove the dry trajectories, we only select back-trajectories with specific humidity ( $q$ ) larger than  $1 \text{ g kg}^{-1}$  along the trajectory at the target region and time.

## Results

### Types of trajectories during AR events



### 1) Illustrative examples

Figure 1. (top rows) MERRA specific humidity ( $q$ ) averaged from the surface up to 700 hPa, the (second and third rows) spatial and temporal evolution of 5-day backward trajectories, and (bottom row)  $q$  values ( $> 1 \text{ g kg}^{-1}$ ) along the trajectories obtained from the nearest location to MERRA  $q$  at each grid point for (a, d, g, j) January 19, 2005; (b, e, h, k) January 14, 1998; and (c, f, i, l) February 16, 2004.

- We designate the first type as Ascending near landfall and of Tropical Origin (AT), the second type as Ascending near landfall and of Extratropical Origin (AE), and the third type as Descending or parallel near landfall and of Extratropical Origin (DE).

### 2) Classification

The majority of AR events (about 86%, 120 out of 140 AR events) over the west coast of the U.S. are associated with three trajectory types.

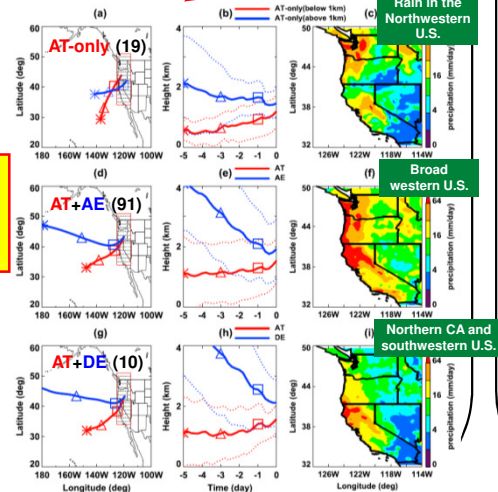


Figure 2. (Left) composite-mean horizontal maps, (middle) vertical evolutions of 5-day back trajectories on 290 K using MERRA reanalysis dataset, and (right) a map of daily precipitation intensity (unit in  $\text{mm day}^{-1}$ ), for (a, b) AT-only, (d, e) AT+AE, and (g, h) AT+DE events.

### Precipitation and AR Trajectories

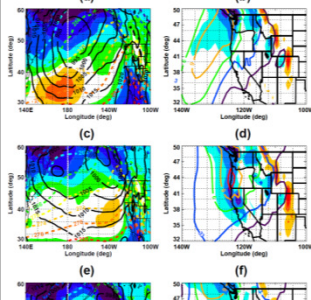
There are different contributions of each trajectory type to precipitation:

- AT-only, AT + AE: associated with high precipitation
- AT + DE: AT are strongly associated with high precipitation than DE
- Heavier precipitation are more associated with AT+AE and AT+DE, emphasizing the extratropical cyclone plays an important role in generating ARs.

- The descending or parallel trajectories (DE) are not typically associated with heavy precipitation. However, given that AT trajectories from AT+DE brings intense precipitation, DE trajectories appear to support in enhancing the updraft from the tropical lower altitude, and resulting in precipitation by AT trajectories.

Figure 3. (a, c, e) PDFs of precipitation corresponding to the mean trajectories, and (b, d, f) percentages of number of events when precipitation is larger than 20 (gridded fill), and 30 (solid fill)  $\text{mm day}^{-1}$  for AT-only (red), AE (blue), and DE (blue) trajectories. The red (blue) lines represent the PDF of precipitation for mean of AT (AE) (above 1km for AT-only), AE, DE) trajectories.

### Characteristics of meteorological fields



- For all events, the minimum surface pressure (less than 990 hPa) from the northern Pacific basin penetrates further southward.

AT-only: a single low pressure center, strong vertical motion over the northwestern coast of the U.S.  
AT+AE, AT+DE: double low pressure centers, making a strong trough-ridge structure, strong updraft over the west coast of the U.S.

Figure 4. Composite-mean (a, c, e) surface pressure (black solid line), zonal velocity (shading), overlaid by temperature (dashed line), and (b, d, f) Composite-mean vertical velocity ( $u$ ,  $\text{Pa s}^{-1}$ , shading, negative value means upward motion) overlaid by meridional velocity (contour), averaged over 700–1000 hPa for (top) AT-only, (middle) AT+AE, and (bottom) AT+DE events.

### Upper level PV and diabatic heating

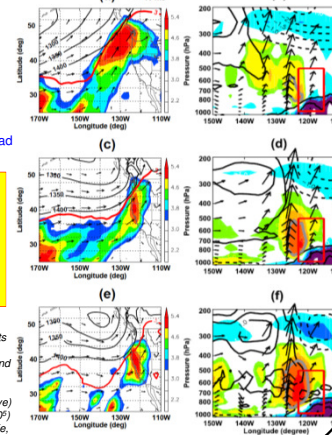


Figure 5. (left panels) composite mean of 850 hPa horizontal wind (vectors), 850 hPa geopotential heights (black solid lines), and specific humidity ( $q$ ) ( $\text{g kg}^{-1}$ ) averaged over 850–700 hPa. PV of 3PVU (red line), and (right panels) composites of total diabatic heating anomalies (shading,  $\text{K day}^{-1}$ ), and potential vorticity anomalies (PV, thick line [PVU], dashed line is negative) from the zonal mean, and wind vector (arrow [ $\text{ms}^{-1}$ ]10°) at the target day for (a, b) AT-only, (c, d) AT+AE, and (e, f) AT+DE events.

### Rossby wave breakings (PV orientation)

Anticyclonic RWB types (79 events) are much more dominant types than the cyclonic RWB types (8 events) – 66% of AR events are associated with anticyclonic Rossby wave breakings

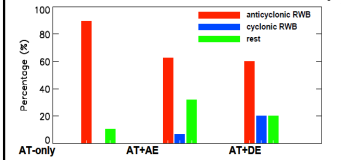


Figure 6. The percentages of the PV orientation for each AR event

### Vertically integrated water vapor fluxes

The vertically integrated water vapor fluxes are large for  
-AT-only: in the northwestern U.S. (ranging from 42–50N).  
-AT+AE: over the broad region of the western U.S.  
-AT+DE: in the southwestern U.S. including California (ranging from 34–42N)

- These are all closely related to the direction of horizontal winds, and the shape of composite-mean upper level PV.

Figure 7. (a, c, e) (left) The composite mean vertically integrated horizontal water vapor fluxes (color and arrows, unit in  $\text{kg m}^{-1} \text{ s}^{-1}$ ) overlaid by PV (2.5 PVU), and (right) the components orthogonal to the coastline for (top) AT-only, (middle) AT+AE, and (bottom) AT+DE events. Vector represents the magnitude of water vapor fluxes (unit in  $\text{kg m}^{-1} \text{ s}^{-1}$ ).

## Summary and Conclusions

- The majority of AR events (86%) in the western U.S. are related to one of the three trajectory types.
- The magnitude and the spatial distribution of precipitation of a given AR event are found to be strongly determined by the type of trajectories. For example,
  - i) AR events composed of both AT and AE trajectories (AT+AE) have more frequent precipitation over a broad region of the western U.S.
  - ii) AR events composed of both AT and DE trajectories (AT+DE) have intense precipitation over the southwestern U.S. due to AT trajectories.
  - li) AR events of AT-only trajectories (AT-only) have intense precipitation, especially over the northwestern U.S., but are less frequent compared to those of AT + AE trajectories.
- Trajectory types are closely linked to diabatic heating and upper-level PV anomalies.
- About 70% of AR events are associated with anticyclonic Rossby wave breaking events.

## References

Neiman, P. J., F. M. Ralph, G. A. Wick, J. D. Lundquist, and M. D. Dettinger (2008), Meteorological Characteristics and Overland Precipitation Impacts of Atmospheric Rivers Affecting the West Coast of North America Based on Eight Years of SSM/I Satellite Observations. *Journal of Hydrometeorology*, 9, 22–47, 2008.

Newell, R. E., N. E. Newell, Y. Zhu, and C. Scott (1992), Tropospheric rivers? A pilot study. *Geophys. Res. Lett.*, 19, 2401–2404.

Ralph, F. M., P. J. Neiman, G. A. Wick, S. I. Gutman, M. D. Dettinger, D. R. Cayan, and A. B. White (2006), Flooding on California's Russian River: The role of atmospheric rivers. *Geophys. Res. Lett.*, 33, L13801, doi:10.1029/2006GL026689.

Ryo, J.-M., D. E. Waliser, D. W. Waugh, S. Wong, E. J. Fetzer, and I. Fung (2015), Classification of atmospheric river events on the U.S. West Coast using a trajectory model. *J. Geophys. Res. Atmos.*, 120, doi:10.1002/2014JD022023.

Schoeberl, M. R., and L. Spurling (1995), Trajectory modeling, in *Diagnostic Tools in Atmospheric Physics*, edited by G. Fiocco and G. Visconti, Proc. Int. Sch. Phys. "Enrico Fermi," 124, 289–306.

Wernli, H., and H. C. Davies (1997), A Lagrangian-based analysis of extratropical cyclones. I: The method and some applications. *Q. J. Meteorol. Soc.*, 123, 467–489.